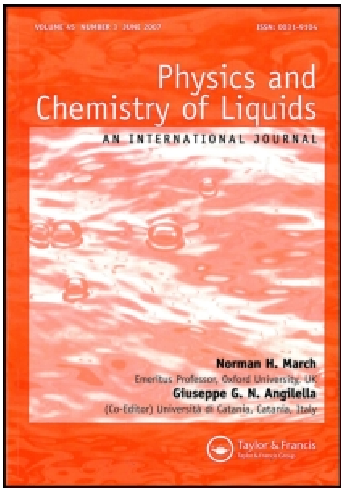

Physics and Chemistry of Liquids
Publication details, including instructions for authors and subscription information:
http://www.informaworld.com/smpp/title~content=t713646857

Phase Transitions Wholly within the Liquid State

G. G. N. Angilella[a]; F. E. Leys[b]; N. H. March[bc]; R. Pucci[a]
[a] Dipartimento di Fisica e Astronomia Università di Catania and Instituto Nazionale per la Fisica della Materia UdR Catania 64 Via S. Sofia I-95123 Catania Italy, [b] Department of Physics University of Antwerp Groenenborgerlaan 171 B-2020 Antwerp Belgium, [c] Oxford University Oxford England,

To cite this Article Angilella, G. G. N. , Leys, F. E. , March, N. H. and Pucci, R.(2003) 'Phase Transitions Wholly within the Liquid State', Physics and Chemistry of Liquids, 41: 3, 211 — 226

To link to this Article: DOI: 10.1080/0031910021000061574

URL: http://dx.doi.org/10.1080/0031910021000061574

Physics and Chemistry of Liquids
2003, Vol. 41, No. (3), pp. 211–226

Review

PHASE TRANSITIONS WHOLLY WITHIN THE LIQUID STATE

G.G.N. ANGILELLA[a,]*, F.E. LEYS[b], N.H. MARCH[b,c] and R. PUCCI[a]

[a]*Dipartimento di Fisica e Astronomia, Università di Catania and Instituto Nazionale per la Fisica della Materia, UdR Catania, 64, Via S. Sofia, I-95123 Catania, Italy;* [b]*Department of Physics, University of Antwerp, Groenenborgerlaan 171, B-2020 Antwerp, Belgium;*
[c]*Oxford University, Oxford, England*

(Received 20 October 2002)

After a quite brief discussion of the quantal liquids ^{4}He, ^{3}He and H, 'classical' elemental liquids which are treated in turn are C, P, Se and S. Phase boundaries in the (p, T) plane exist for each of these liquids, characterized by a change in local coordination number across these boundaries. Corresponding changes in other physical properties are briefly noted. Finally, following this review of elemental liquids, some liquids with two types of atom are briefly considered, the most important but also the most controversial being water.

Keywords: Liquid–liquid phase transitions

1 BACKGROUND AND OUTLINE

The era of phase transitions wholly within the liquid state probably began with the discovery of the superfluid transition in liquid ^{4}He. We shall therefore start this review with quantal liquids, though the most recent work we shall summarize is concerned with essentially classical liquids.

The outline of the review can then be stated very briefly as follows. In Section 2, liquid ^{4}He, liquid ^{3}He and liquid hydrogen are considered in turn, the phase transition discussed in liquid hydrogen being a molecular–insulator to molecular–metal transition, following the pioneering work of Weir *et al.* [1]. Then elemental 'classical' liquids are reviewed (see also [2]), prominence being given to a liquid–liquid phase transition (LLPT) in carbon, and to the related experiments of Togaya [3] on the melting line of graphite and to the atomistic simulations of Glosli and Ree [4]. These aspects are dealt with in Section 3, while Section 4 consists of a briefer discussion of molten Se and S. After a short summary of diffraction experiments on phosphorus, followed by an account of some simulations of liquid phosphorus by Hohl and Jones [5]

---

*Corresponding author. Fax: + 39 095 378 5231. E-mail: Giuseppe.Angilella@ct.infn.it

ISSN 0031-9104 print: ISSN 1029-0451 online
DOI: 10.1080/0031910021000061574

(Section 5), some attention is given to very recent work on water [6–8] in Section 6. The final Section constitutes a summary with some proposals set out for future studies that may prove fruitful. In an Appendix, a simple theoretical model proposed by Lee and Swendsen [9] is reviewed, based on a Lennard–Jones 6–12 interaction but modified to allow for the possibility of different types of short-range orientational order in materials in which a LLPT may occur.

2 PHASE TRANSITIONS IN QUANTAL LIQUIDS

2.1 Liquid ^{4}He

Dramatic experiments, such as the fountain effect discovered by Allen and Misener [10], on liquid ^{4}He may have been the origins of phase transitions occurring wholly within the liquid state. At perhaps a more mundane level, as the liquid was cooled down to 2.2 K, the hitherto bubbling liquid became quiescent. Lynton [11] likened the behaviour to a 'thermal superconductor'. Other evidence was the λ-like behaviour of the specific heat as the liquid was cooled through 2.2 K.

In pioneering work, Penrose and Onsager [12] pressed the analogy with Bose–Einstein condensation in a vapour. However, they recognized that the condensate density would be low (their estimate was $\sim 10\%$). Both neutron experiments [13] and diffusion quantum Monte Carlo simulations [14] have been carried out quite recently and yield a somewhat lower condensate density $\sim 7\%$.

Though the LLPT from 'normal' to superfluid is completely established by experiment, it is hard to understand how the phenomenon of superfluidity is 'driven' by such a small condensate fraction (see also [15]), in contrast to the very recent experiments on trapped atomic vapours [16], where the condensate fraction is essentially unity.

It is relevant therefore to point out (see, e.g. the experiments of Grisenti *et al.* [17]) that it is possible that *n*-mers of ^{4}He atoms may play a role (see [18–20], for a discussion of the possible role of dimers and trimers in the phenomenon of superfluidity in liquid ^{4}He). But this could, perhaps, herald a further LLPT at the lowest feasible temperatures, between two superfluid phases in which basically different mechanisms of superfluidity obtain.

To end this very brief account, a LLPT in ^{4}He is established beyond doubt, from a 'normal' liquid to a superfluid state: this may be the first time a LLPT was observed.

2.2 Liquid ^{3}He

We turn now to the more recent discoveries of phases of liquid ^{3}He, built up now, of course, from Fermionic atoms. Figure 1 shows early specific heat measurements made by Webb *et al.* [21]. The shape of this curve is in fact characteristic of a 'Bardeen–Cooper–Schrieffer'-like pairing transition.

The complete phase diagram of liquid ^{3}He is quite complex, as a *p*–*T*–*H* diagram is required, with *H* an applied magnetic field. Experimental data of Paulson *et al.* [22] are shown in Fig. 2, which is redrawn from Fig. 11 of [23]. This work of Paulson [22] on the phase diagram in a magnetic field was an investigation at pressures below melting pressure, in which a study was made of the static magnetization of the liquid via superconducting quantum interference device (SQUID) interferometry. As Lee [23]

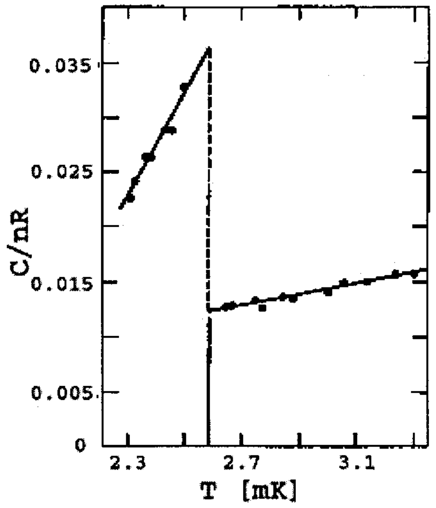

FIGURE 1 Specific heat measurements of liquid ^{3}He-*A* near the superfluid transition, at $p = 33.41$ bar. Redrawn from Webb *et al.* [21].

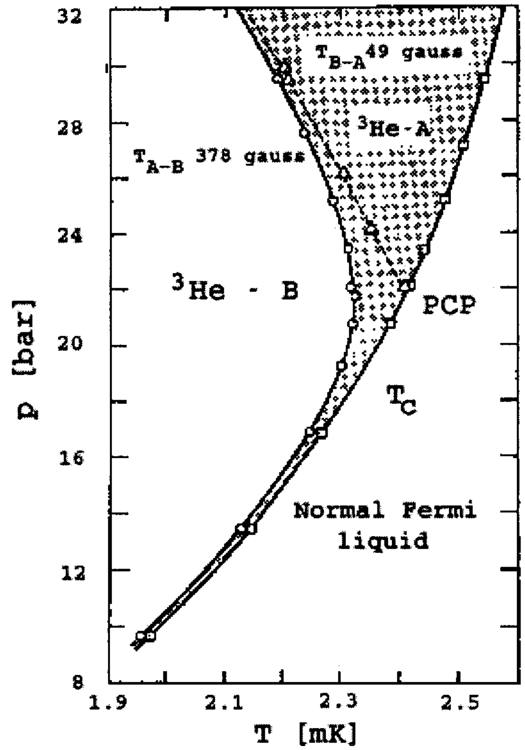

FIGURE 2 Experimental data of Paulson *et al.* [22] showing *p*–*T* diagram of liquid ^{3}He in a magnetic field. At the lowest magnetic field, the *A* phase is not present below polycritical point PCP at about 22 bar. With increasing magnetic field, *B* phase is suppressed in favour of *A* phase even at the lowest pressure, and PCP disappears. Redrawn from Lee [23].

stresses, their most dramatic finding was the narrowing, and eventually the vanishing, of the phase labelled *A* in Fig. 2 in zero field at a point labelled PCP (polycritical point) in this figure. For more details, the reader should consult the article by Lee [23], who summarizes the features discussed above in a schematic *p–T–H* diagram in his Fig. 12.

As Lee [23] points out, the phenomena discussed above have relevance to astrophysics. The pairing state (*p*-wave) in superfluid ^{3}He referred to above in relation to the specific heat behaviour in Fig. 1, may have relevance to possible pairing behaviour in neutron stars. Lee [23] also suggests that the superfluid phase transitions in ^{3}He which have been briefly reviewed above may serve as a possible model for transitions which may have occurred in the early Universe.

To complete this quite brief Section on quantal liquids, we turn finally to the case of liquid molecular hydrogen.

2.3 Phase Diagram of Liquid Hydrogen, Including a Molecular Insulator–Molecular Metal LLPT

In early work by Leung *et al.* [24], a schematic (only) phase diagram for hydrogen was proposed, which is redrawn in Fig. 3.

Exciting additions to this schematic diagram have been made, both by experiment [1] and by path integral quantum Monte Carlo simulations [25]. The conclusion reached from the experiment of Weir *et al.* [1] is that liquid molecular hydrogen in its insulating phase undergoes a transition to a molecular metallic phase at ~1.5 Mbar. Arguments of a thermodynamic character indicate that substantially higher pressures will be needed to produce molecular metallic solid hydrogen – which remains a central aim of high pressure physics.

Weir *et al.* [1] found that the magnitude of the electrical conductivity in the molecular metallic liquid was comparable to that, for example, in expanded liquid metal Rb.

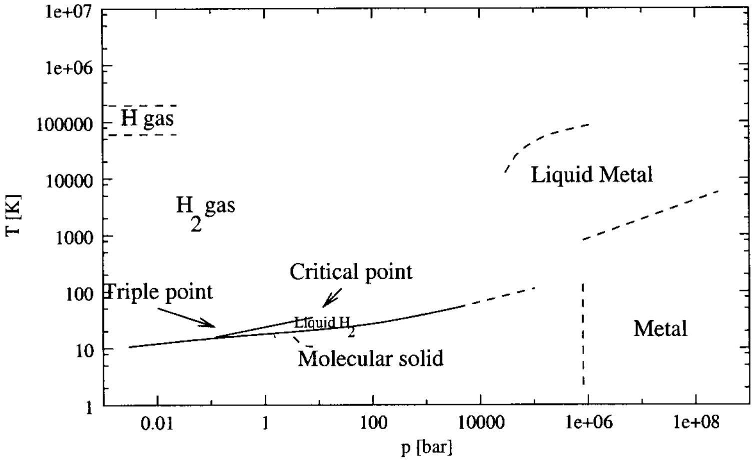

FIGURE 3 Schematic phase diagram of hydrogen, showing liquid–vapour critical point. Redrawn from Leung *et al.* [24].

Returning to the quantal computer studies of Magro *et al.* [25] over an extremely wide range of thermodynamic states, March and Tosi [26] have modelled their data in a semiquantitative fashion using in appropriate ranges an H_2 molecule in a suitable box or, when dissociation occurs, a H atom in a confining sphere. But what is presently lacking on the theoretical side is to use Kubo–Greenwood theory of electrical transport to examine when one enters, under the extremely high pressure cited above, the molecular metallic phase of liquid hydrogen.

The final comment here is that these considerations on molecular metallic hydrogen are extremely relevant to discussions on the structure of brown dwarfs. It would take us too far from our main theme to go into details here, but the interested reader is referred to the work of Hubbard *et al.* [27] and references therein (see also [28]). Suffice it to end this section by saying that the critical point predicted by Saumon and Chabrier [29,30] by a chemical model, and subsequently refined in the quantal Monte Carlo study of Magro *et al.* [25] is an essential ingredient in this area of current astrophysical interest.

3 PHASE TRANSITION IN LIQUID CARBON

Some attention will be devoted below to a LLPT in carbon. As proposed in the early investigation of Ferraz and March [31], *sp* hybridization is eventually to be expected in the low-density liquid, and the breakthrough in this area has been made in the atomistic simulations of Glosli and Ree [4], following the important experiment by Togaya [3].

The work of Glosli and Ree [4] rests on the combination of atomistic simulation techniques and the bond-order potential constructed by Brenner [32–34]. The first quantitative theory that studied the existence of a LLPT was a semiempirical equation of state modelling of molten C by Van Thiel and Ree [35,36]. But as Glosli and Ree [4] emphasize, it was not until 1997 that Togaya [3] published the first experimental evidence for the LLPT in C. Togaya's achievement was to determine the melting line of graphite, and also the electrical resistivity of liquid carbon along this melting curve, by carrying out flash-heating experiments on graphite at high pressures. His finding was that the melting temperature of graphite was enhanced from 4650 K at 1.4 GPa to a maximum of 4790 K at 5.6 GPa, with a subsequent reduction to 4640 K at 9.4 GPa. As to the electrical resistivity, Togaya found that it decreased from 900 to 600 μΩ cm with the above pressure increase. He noted in this publication that changes in slope of the melting curve, and also of the resistivity around 5.6 GPa, were likely fingerprints of a first-order phase transition in liquid carbon.

The above was then the background to the pioneering work of Glosli and Ree [4] employing atomistic simulation methods. To describe the carbon–carbon interaction, the hydrocarbon model potential devised by Brenner [33] was utilized by these authors. This interaction is a member of a class of empirical bond-order potentials (see also [37]) and has the form:

$$\Phi = \sum_{\{\text{bonds}\}} \left[\phi^{\mathrm{R}}(r_{ij}) - b_{ij}\phi^{\mathrm{A}}(r_{ij})\right]. \tag{1}$$

In this Eq. (1), ϕ^{R} and ϕ^{A} denote respectively exponential functions representing the repulsive and attractive terms in the bond energy. The {bonds} symbol in Eq. (1) represents the set of all bonds but it must be stressed that although a sum over bond energies, Φ is not of pair-potential form. The bond-order term b_{ij} has many-body character and depends on both bond and torsional angles, bond lengths and also atomic coordination in the neighbourhood of the bond.

Before making contact between the Glosli–Ree [4] results and the experimental melting line of graphite as measured by Togaya [3], it is important in the context of the present Review to emphasize the nature of the order parameter as proposed by Glosli and Ree [4].

3.1 Glosli and Ree Proposal of the Order Parameter of LLPT Transition in Carbon

Figure 3 of the study of Glosli and Ree [4] shows 'snapshots' of both the low and high density liquids (LDL and HDL) at densities on the phase boundary. They stress that the LDL phase is dominantly *sp*-like in structure, with but little sp^3 hybridization in evidence. In marked contrast, the HDL phase consists mainly of sp^3 bonded atoms.

The proposal of Glosli and Ree is that the order parameter of the LLPT, Ψ say, is

$$\Psi = (\rho_4 - \rho_2)/(\rho_4 + \rho_2), \tag{2}$$

where ρ_2 and ρ_4 denote respectively the number densities of two-fold and four-fold coordinated atoms: this being then a measure of local order. Thus, $\Psi = 1$ if there is no two-fold coordination, and $\Psi = -1$ when no four-fold coordination is found. Their order parameter Ψ is redrawn in the present Fig. 4 as a function of pressure, for four temperatures from 6000 to 9000 K.

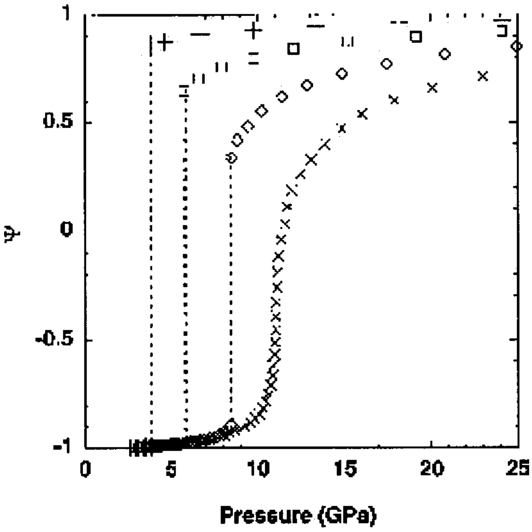

FIGURE 4 Glosli and Ree's proposal for the order parameter Ψ of the LLPT in carbon, Eq. (2) [4], as a function of pressure (+, $T = 6000$ K; □, $T = 7000$ K; ◇, $T = 8000$ K; ×, ◇$T = 9000$ K). Redrawn from Glosli and Ree [4].

3.2 Comments on Absence of an sp^2-liquid phase

To answer the question that arises naturally concerning the absence of an sp^2 liquid phase, Glosli and Ree emphasize that it is important to consider the entropy of the different fluid phases [4]. Then at low pressure it becomes clear that the linear chain structures (sp hybridization) are stabilized with respect to sp^2 or sp^3 hybridized states. At higher pressures, this sp phase must eventually be replaced by higher density phases dominated either by sp^2 or sp^3 hybrids. Glosli and Ree [4] then note that the σ bond in the sp^3 liquid allows for practically free rotations about the bond of the local tetrahedral structures, leading to many conformations energetically nearly the same and high entropy. However, as these authors point out, $\sigma\pi$ bond in the sp^2 phase has a high rotational energy barrier. This favours the planar structure, which then leads to much smaller entropy than for the sp^3 phase. Thus Glosli and Ree conclude that such low entropy results in the sp^2 phase being unfavourable thermodynamically compared with the sp or sp^3 liquid phases.

3.3 Relation of Glosli–Ree Numerical Simulations to Togaya's Experiment

To conclude this section on the LLPT in carbon, we return to the issues discussed in relation to Togaya's measurements on the melting curve of graphite [3]. Figure 5 shows the phase diagram of carbon, experiments of Bundy [38,39] as well as of Togaya [3] being embodied by Glosli and Ree [4], from whose study the figure has been redrawn. The boundary ending in the marked critical point is that across which the LLPT occurs. From the atomistic simulations of Glosli and Ree [4], the critical constants are estimated as $T_c = 8800\,\text{K}$, $p_c = 10.6\,\text{GPa}$, and $V_c = 8.7\,\text{Å}^3/\text{atom}$. This leads to the value of the critical compressibility ratio $Z_c = p_c V_c / k_B T_c = 0.76$.

To refine the simulations, which is necessary as seen from Fig. 5 if fully quantitative agreement is eventually to be obtained with Togaya's melting curve, Glosli and Ree

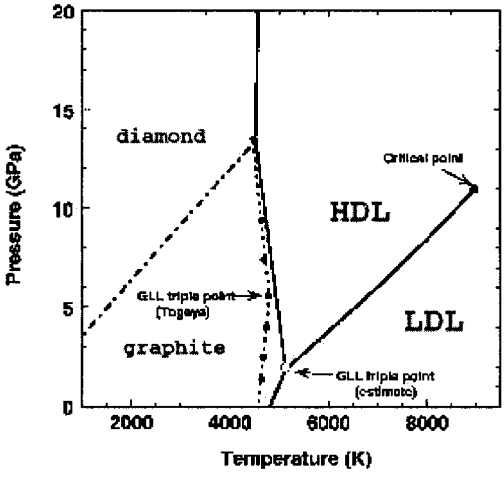

FIGURE 5 p–T diagram of carbon, showing critical point at end of liquid–liquid 'phase boundary'. Dash-dotted line shows experimental results from [38,39]. Dashed line shows experimental results from [35,36]. Continuous lines are simulation results using Brenner potential (see Eq. (1)) [4]. Redrawn from Glosli and Ree [4].

stress that refinements of the bond order potential, Eq. (1), will be needed, and especially these authors emphasize that the inclusion of long-range van der Waals interactions may prove of importance in this context.

While on the properties of elemental carbon, various authors have studied a (as yet hypothetical!) liquid of C_{60} buckyballs, a recent contribution with earlier references being that of Alonso *et al.* [40]. Though as yet of academic interest, it may be interesting for the future to study whether a LLPT could occur in such a liquid!

4 PHASE TRANSITIONS IN Se AND IN S

Below, a brief summary will be presented of related properties of the molten elements Se and S to the LLPT for C discussed immediately above. What will be stressed here is the connection between p–T diagrams of these two elements and measurements of resistance and volumetric anomalies in the liquid phases. The report by Brazhkin *et al.* [41] (see also references therein and [42]) contains fuller experimental details which the interested reader should consult.

4.1 Molten Se

The short-range order in molten Se is characterized by two-fold coordination, just as for the crystal. But the structure of Se grossly changes on changing the temperature T. More specifically, increasing T substantially reduces the mean molecular chain length. As an illustration, in the neighbourhood of the liquid–gas critical point, with critical constants given by $T_c = 1630°\mathrm{C}$, $p_c = 380$ bars, and $d_c = 1.85\,\mathrm{g/cm^3}$, with critical compressibility ratio $Z_c = 0.10$, the average chain molecule is built from only ~ 10 atoms [43].

The measurements currently available on the liquid structure factor $S(k)$ show plainly marked differences at pressures of 4.4 and 8.4 GPa from what is found at normal pressure. Put another way, a major structural transformation can be brought about in liquid Se by substantial compression.

In the present context of LLPT, it is also significant that both electrical and volumetric anomalies in molten Se have been detected experimentally in the pressure regime between 1 and 10 GPa [44]. The p–T diagram according to Brazhkin *et al.* [41] is redrawn in Fig. 6: all the findings summarized above are consistent with a structural transformation taking place across the boundary separating the two phases L and L$'$ marked on this figure.

4.2 Molten S

Turning to elemental molten sulphur, once again there occur structural modifications which are brought about by increasing the temperature T at atmospheric pressure. Adjacent to the melting temperature of 390 K, the short-range order in the melt still reflects that in the solid phase, and is described in terms of the same S_8 rings. According to Meyer [45], one can regard sulphur in this regime as built from such S_8 rings as structural units with an average bond length of 2.05 Å and an angle of $\sim 108°$. The melting temperature is $\sim 115°\mathrm{C}$ and sulphur is in the form of a light yellow liquid having a relatively low viscosity. At a temperature near 160°C, the

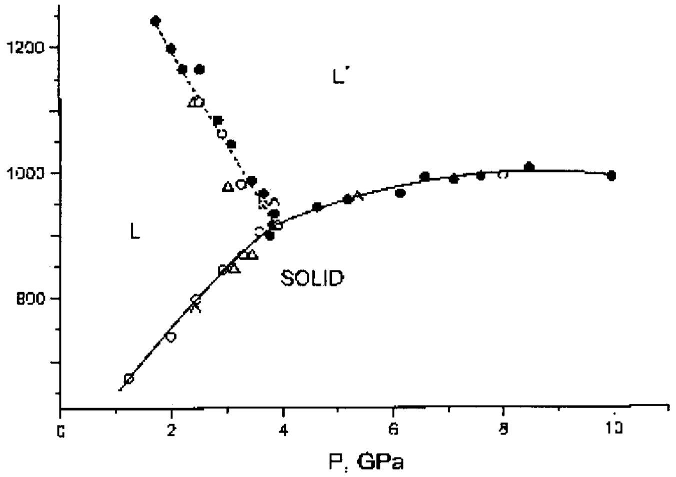

FIGURE 6 p–T diagram of solid and liquid Se. L and L′ denote the liquid phases. Redrawn from Brazhkin *et al.* [41].

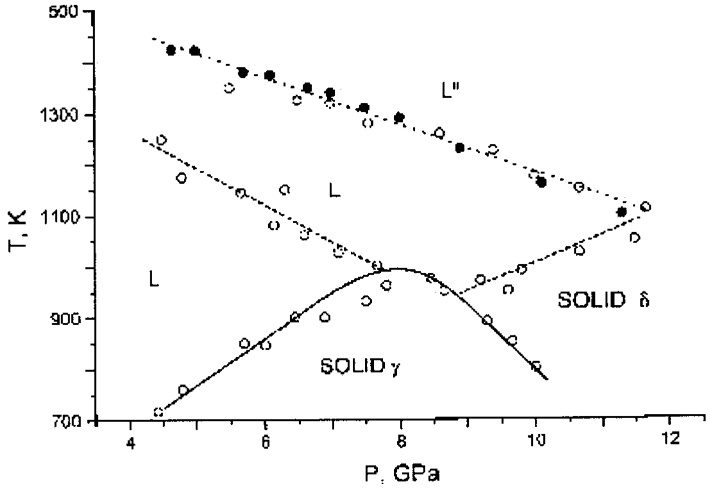

FIGURE 7 p–T diagram of solid and liquid sulphur. L, L′ and L'' denote the liquid phases. γ and δ denote the solid phases. Redrawn from Brazhkin *et al.* [41].

viscosity of the liquid then increases markedly. Since viscosity can be (of course approximately) related to the structure factor $S(k)$ via intermolecular forces, further studies of this structural phase transition would probably prove fruitful. Then, in this same context, it is noteworthy that Duda and Holovo [46] has gained some insight into $S(k)$ for liquid sulphur via an analytical solution of the polymer Percus–Yevick equation utilizing the fused hard sphere polyatomic model. Motivation, at least in part, for their study of the equilibrium structure factor of elemental sulphur, was the importance of these macromolecules in the chemical industry.

A p–T diagram of liquid and solid S is shown in Fig. 7, redrawn from the work of Brazhkin *et al.* [41].

In closing this section, it is noteworthy that Hohl and Jones [47] have presented results of a molecular-dynamics simulation of liquid and amorphous Se. In particular, pair correlation functions and corresponding structure factors $S(k)$ were computed.

5 EXPERIMENTS AND THEORY ON LIQUID PHOSPHORUS: EVIDENCE FOR A LLPT

The plethora of solid-state structures exhibited by phosphorus means that its chemical bonding propensities are among the most fascinating of the elements in the Periodic Table, only sulphur, selenium (see also Section 4) and boron displaying a comparable variety of structures. One relevant solid-state assembly is a molecular crystal (white P) comprising tetrahedral P_4 units, and there are a variety of 'red' forms, the latter being usually amorphous.

If the molecular insulator, white P, is heated above its melting point (315 K), the resultant liquid phase is also built up of tetrahedral P_4 molecules with bond length 2.210 Å [48,49]. Such neutron diffraction studies reveal, in spite of 'almost spherical' P_4 building blocks, considerable intermediate range order (~20 Å). This indicates orientational ordering of the tetrahedra. It also turns out that highly pure liquid P can be held in a stable, supercooled state more than 100 K lower than its melting temperature. This appears to be possible for much longer than other liquids [50] and the spatial correlations seem similar at $T = 323\,\mathrm{K}$ and in the supercooled liquid at 283 K [48,49].

But, more specifically, X-ray diffraction evidence for a LLPT in phosphorus has been reported quite recently by Katayama *et al.* [51] (see also Fig. 8, redrawn from [51]).

We turn from experimental observations to summarize some findings from the important computer simulation study of Hohl and Jones [5]. Their investigations were carried out by the molecular-dynamics – density functional method. They started out from a system of 26 P_4 tetrahedra in a simple cubic unit cell of constant volume. They then determined radial, angular and defect distribution functions for the molecular liquid and also for polymeric high temperature red P in the molten state. They conclude by comparison with available experiments that the atomic structure factors of amorphous and liquid polymeric phases are quite similar. They present evidence

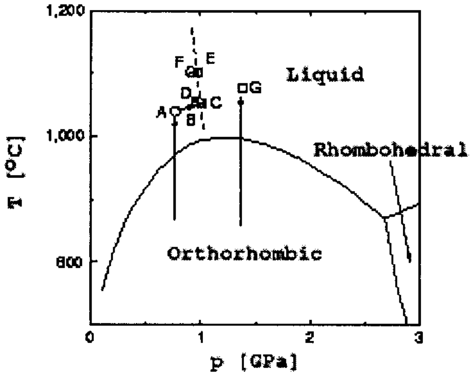

FIGURE 8 p–T diagram of solid and liquid phosphorus. Redrawn from Katayama *et al.* [51].

that the polymerization of molecular phosphorus is a complex process that may be regarded as a defect-induced chain reaction. In this process, they conclude that elevated temperature and the environment of the tetramers have major roles. The interested reader is referred to their original articles for full details [5] (see also [52]).

6 EVIDENCE FOR A LLPT IN WATER

A great deal of work has been carried out on the phase diagram of water and the connection among its liquid, supercooled and glassy phases (see, e.g. [53–56]).

We shall focus here predominantly on the very recent study of Yamada *et al.* [6,57], who employ the water model proposed by Mahoney and Jorgensen [7,8], which appears to exhibit properties of water more realistically than earlier pairwise additive force fields.

As Yamada *et al.* [6] stress, their objective was to unify phenomena connected with the existence of a LLPT and homogeneous nucleation via a molecular dynamics simulation. In particular, these authors simulate a system of 343 molecules interacting with the transferable intermolecular potential with five points (TIP5P) [7,8]. The TIP5P force field reproduces the density anomaly at 1 atm and provides excellent structural data when compared with experiment (see also [58]). Under ambient conditions, the diffusion constant is given in good agreement with the experimental result, while away from ambient conditions the temperature and pressure dependence are reasonably reproduced.

In Fig. 9, results of Yamada *et al.* [6] are displayed for the pressure along isotherms. It can be seen that, on lowering the temperature, an inflexion is detected, which

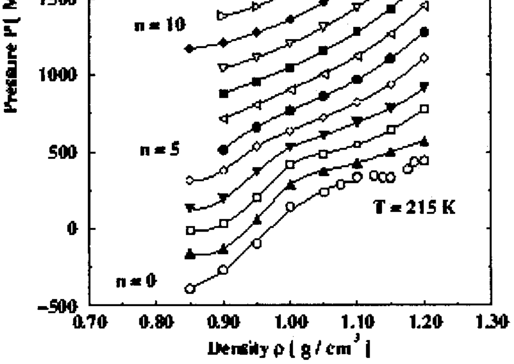

FIGURE 9 Pressure as a function of density along several isotherms in water. Each curve has been shifted by $n \times 150$ MPa. Redrawn from Yamada *et al.* [6].

eventually yields a flat isotherm at the lowest temperature shown ($T = 215\,\mathrm{K}$). This 'flat' coexistence region, in the study of Yamada *et al.* [6], indicates the presence of a LLPT.

Yamada *et al.* emphasize that experimental measurements of metastable liquid states are strongly influenced by homogeneous nucleation. The nucleation and growth of ice particles from aqueous solution has been widely investigated (see [53], and also [59,2]). Yamada *et al.* [6] point out that the non-monotonic relation between crystallization rate and supercooling depth arises from competition between 'the thermodynamic driving force for nucleation and the viscous slowing down' (see again [53]). Crystallization is a hindrance to direct experimental investigation of pure metastable liquid H_2O below the homogeneous nucleation line: only indirect measurements being feasible, by studying the metastable melting lines of ices [60,61].

7 SUMMARY AND FUTURE DIRECTIONS

A substantial field is evidently developing now concerned with LLPTs. While, as set out in Section 1, its origin probably lies in the superfluid transition in liquid ^{4}He, experimental evidence can leave little doubt that in elemental 'classical' liquids, such an LLPT is now pretty firmly established in liquid C, in both liquid Se and S, and in liquid P. Probably the most detailed investigations to date centre round liquid C, where the phase diagram is now established in at least semi-quantitative detail. The work on liquid water, the only material we have considered in this review built from more than one type of atom, is potentially of great interest, but what aspects one can hope to observe experimentally is a topic needing further clarification.

As to future directions, we confine ourselves below to isolating a few specific topics on particular materials considered above. Thus we single out:

1. Important refinements of the phase diagram of C await the possibility of transcending the Brenner bond-order potential and in particular investigating the consequences of incorporating long-range van der Waals interactions (see also Glosli and Ree [4]). Of course, further experimental work following Togaya [3] would also be important but access to the relevant thermodynamic states has imposed severe restrictions to date.
2. Liquid P, with its very versatile chemical bonding propensities, seems to be another material where further experimental work is of some urgency, both structurally and also involving atomic transport. Contact between computer simulation [5] and the recent X-ray diffraction experiments [51] is also an area of continuing interest.
3. The liquid phase of hydrogen remains, of course, a problem of great interest. Kubo-like study of the electrical conductivity of phases already considered by Magro and Ceperley [25] remains a matter of outstanding interest for the future.

NOTES ADDED IN PROOF

Y. Katayama [*J. Non-Cryst. Solids* **312–314**, 8 (2002)] has reported on abrupt pressure-induced change between two distinct forms of liquid P at roughly 13 GPa by an X-ray diffraction study. This suggests the low pressure form is a liquid of largely uncorrelated P_4 molecules. Indications are reported that the high-pressure form has a polymeric structure.

Complementary first-principle MD simulations of liquid P were reported in the same journal [Y. Senda, F. Shimojo, and K. Hoshino, *J. Non-Cryst. Solids* **312–314**, 80 (2002)].

A. Botti, F. Bruni, A. Isopo, M. A. Ricci, A. K. Soper [*J. Chem. Phys.* **117**, 6196 (2002)] recently presented neutron diffraction data on three isotopically substituted samples of liquid water in the supercooled regime ($T = 267\,\mathrm{K}$, $\rho = 100.2\,\mathrm{atoms/nm}$). These results are compatible with previous X-ray experiments, and allowed to extract the partial radial distribution functions for bulk water in this regime for the first time.

The phase diagram of water in the supercooled regime has been theoretically investigated by N. Guisoni, V. B. Henriques [*J. Chem. Phys.* **115**, 5238 (2001)], who performed a mean-field analysis of Bernal's geometric model for liquids in two dimensions.

Liquid polymorphism has been reported in the organic liquid triphenyl phosphite [A. Ha, I. Cohen, X.-L. Zhao, M. Lee, and D. Kivelson, *J. Phys. Chem.* **100**, 1 (1996); see also [2]].

A final area, but now more speculative and of longer term interest perhaps, is to understand the phase behaviour of water in high electric fields. We mention here (i) the observation by Y. S. Chu, T. E. Lister, W. G. Cullen, H. Zou, Z. Nagy, *Phys. Rev. Lett.* **86**, 3364 (2001), of phase transitions in a few molecular H_2O layers at a RuO_2 electrode due to high electric fields and (ii) the model approach of I. Danielewicz-Ferchmin and A. R. Ferchmin, *Chem. Phys. Lett.* **351**, 397 (2002), via which indications are found that a phase transition between partly orientationally ordered water and a different phase of H_2O orientationally ordered at a moleculare level might occur at a local field strength of $10^9\,\mathrm{V\,m^{-1}}$.

Acknowledgements

F.E.L. thanks Professor K. Van Alsenoy for much motivation and encouragement, while N.H.M. is indebted to Professor M.P. Tosi for invaluable discussions on the general area embraced by this article. F.E.L. also acknowledges financial support from the "Program for the Stimulation of Participation in Research Programs of the European Union" of the University of Antwerp. Finally, N.H.M. and F.E.L. thank the Department of Physics and Astronomy, University of Catania, for the stimulating environment and much hospitality.

References

[1] S.T. Weir, A.C. Mitchell and W.J. Nellis (1996). *Phys. Rev. Lett.*, **76**, 1860.
[2] P.H. Poole, T. Grande, C.A. Angell and P.F. McMillan (1997). *Science*, **275**, 322.
[3] M. Togaya (1997). *Phys. Rev. Lett.*, **79**, 2474.
[4] J.N. Glosli and F.H. Ree (1999). *Phys. Rev. Lett.*, **82**, 4659.
[5] D. Hohl and R.O. Jones (1994). *Phys. Rev. B*, **50**, 17047.
[6] M. Yamada, S. Mossa, H.E. Stanley and F. Sciortino (2002). *Phys. Rev. Lett.*, **88**, 195701.
[7] M.W. Mahoney and W.L. Jorgensen (2000). *J. Chem. Phys.*, **112**, 8910.
[8] M.W. Mahoney and W.L. Jorgensen (2001). *J. Chem. Phys.*, **114**, 363.
[9] H.K. Lee and R.H. Swendsen (2001). *Phys. Rev. B*, **64**, 214102.
[10] J.F. Allen and A.D. Misener (1938). *Nature* (London), **141**,75.

[11] E.A. Lynton (1964). *Superconductivity*. Methuen, London.
[12] O. Penrose and L. Onsager (1956). *Phys. Rev.*, **104**, 576
[13] H.R. Glyde, R.T. Azuah and W.G. Stirling (2000). *Phys. Rev. B*, **62**,14337.
[14] S. Moroni, G. Senatore and S. Fantoni (1997). *Phys. Rev. B*, **55**, 1040.
[15] A. Minguzzi, N.H. March and M.P. Tosi (2002). in course of publication.
[16] E.A. Cornell and C.E. Wieman (2002). *Rev. Mod. Phys.*, **74**, 875.
[17] R.E. Grisenti, W.Schöllkopf, J.P. Toennies, G.C. Hegerfeldt, T. Köhler and M. Stoll (2000). *Phys. Rev. Lett.,* **85**, 2284.
[18] N.H. March (1983). *J. Chem. Phys.*, **79**, 529.
[19] N. H. March (1984). *J. Chem. Phys.*, **81**, 587.
[20] H. Ghassib and G.V. Chester, (1984). *J. Chem. Phys.*, **81**, 585.
[21] R.A. Webb, T.J. Greytak, R.J. Johnson and J.C. Wheatley (1973). *Phys. Rev. Lett.*, **30**, 210.
[22] D.N. Paulson, H. Kojima and J.C. Wheatley (1974). *Phys. Rev. Lett.*, **32**, 1098.
[23] D.M. Lee (1997). *Rev. Mod. Phys.*, **69**, 645.
[24] W.B. Leung, N.H. March and H. Motz (1976). *Phys. Lett. A*, **56**, 425.
[25] W.R. Magro, D.M. Ceperley, C. Pierleoni and B. Bernu (1996). *Phys. Rev. Lett.*, **76**, 1240.
[26] N.H. March and M.P. Tosi (1996). *Nuovo Cimento D*, **18**, 1061.
[27] W.B. Hubbard, J.J. Fortney, J.I. Lunine, A. Burrows, D. Sudarsky and P. Pinto (2001). *Astrophys. J.*, **560**, 413.
[28] G. Chabrier, D. Saumon, W.B. Hubbard and J.I. Lunine (1992). *Astrophys. J.*, **391**, 817.
[29] D. Saumon and G. Chabrier (1991). *Phys. Rev. A*, **44**, 5122.
[30] D. Saumon and G. Chabrier (1992). *Phys. Rev. A*, **46**, 2084.
[31] A. Ferraz and N.H. March (1979). *Phys. Chem. Liquids*, **8**, 289.
[32] D.W. Brenner (1990). *Phys. Rev. B*, **42**, 9458.
[33] D.W. Brenner (1992). *Phys. Rev. B*, **46**, 1948.
[34] D.W. Brenner (2000). *Physica Status Solidi (b)*, **217**, 23.
[35] M. Van Thiel and F.H. Ree (1993). *Phys. Rev. B*, **48**, 359.
[36] M. Van Thiel and F.H. Ree (1995). *J. Appl. Phys.*, **77**, 4804.
[37] G.G.N. Angilella, A. Grassi, G.M. Lombardo, N.H. March and R. Pucci (2001). In: S.G. Pandalai (Ed.), *Recent Research Developments in Quantum Chemistry*, Vol. 2, p. 9. Transworld Research Network, Trivandrum, India.
[38] F.P. Bundy (1963). *J. Chem. Phys.*, **38**, 618.
[39] F.P. Bundy (1963). *J. Chem. Phys.*, **38**, 631.
[40] J.A. Alonso, M.J. López, N.H. March and D. Lamoen (2002). *Phys. Chem. Liquids*, **40**, 457.
[41] V.V. Brazhkin, S.V. Popova and R.N. Voloshin (1999). *Physica B*, **265**, 64.
[42] G.G.N. Angilella, R. Pucci, G. Piccitto and F. Siringo (Eds.) (1999). *Molecular and Low Dimensional Systems under Pressure. Proceedings of the XXXVI EHPRG Meeting*, Vol. 265 of *Physica B*. North Holland, Amsterdam.
[43] H. Endo, K. Tamura and M. Yao (1987). *Can. J. Phys.*, **65**, 266.
[44] V.V. Brazhkin, R.N. Voloshin and S.V. Popova (1989). *Piz'ma Zh. ETF*, **50**, 424.
[45] B. Meyer (1965). *Elemental Sulphur*. Interscience, New York.
[46] Y. Duda and M.F. Holovo (1997). *Phys. Chem. Liquids*, **35**, 175.
[47] D. Hohl and R.O. Jones (1991). *Phys. Rev. B*, **43**, 3856.
[48] J.H. Clarke, J.C. Dore, J.R. Granada, J. Reed and G. Walford (1981). *Mol. Phys.*, **42**, 861.
[49] J.R. Granada and J.C. Dore (1982). *Mol. Phys.*, **46**, 757.
[50] J.H. Hildebrand and G.J. Rotarin (1951). *J. Am. Chem. Soc.*, **73**, 2524.
[51] Y. Katayama, T. Mizutani, W. Utsumi, O. Shimomura, M. Yamakata and K. Funakoshi (2000). *Nature*, **403**, 170.
[52] D. Hohl and R.O. Jones (1992). *Phys. Rev. B*, **45**, 8995.
[53] P.G. Debenedetti (1996). *Metastable Liquids*. Princeton University Press, Princeton.
[54] O. Mishima and H.E. Stanley (1998). *Nature*, **392**, 164.
[55] O. Mishima and H.E. Stanley (1998). *Nature*, **396**, 329.
[56] V. Velikov, S. Borick and C.A. Angell (2001). *Science*, **294**, 2335.
[57] N. Giovambattista, F.W. Starr, F. Sciortino, S.V. Buldyrev and H.E. Stanley (2002). *Phys. Rev. E*, **65**, 041502.
[58] G. Hura, J.M. Sorensen, R.M. Glaeser and T. Head-Gordon (2000). *J. Chem. Phys.*, **113**, 9149.
[59] D.R. MacFarlane, R.K. Kadiyala and C.A. Angell (1983). *J. Chem. Phys.*, **79**, 3921.
[60] O. Mishima (1994). *J. Chem. Phys.*, **100**, 5910.
[61] O. Mishima, (2000). *Phys. Rev. Lett.*, **85**, 334.
[62] G. Stell and P.C. Hemmer (1972). *J. Chem. Phys.*, **56**, 4274.
[63] P.C. Hemmer and G. Stell (1970). *Phys. Rev. Lett.*, **24**, 1284.
[64] M.R. Sadr-Lahijany, A. Scala, S.V. Buldyrev and H.E. Stanley (1998). *Phys. Rev. Lett.*, **81**, 4895.
[65] G. Franzese, G. Malescio, A. Skibinsky, S.V. Buldyrev and H.E. Stanley (2001). *Nature*, **409**, 692.

APPENDIX

LEE–SWENDSEN MODEL OF LIQUID–LIQUID PHASE TRANSITIONS

Stell and Hemmer [62,63] in early work demonstrated the existence of a LLPT in a one-dimensional model based on a softened hard core potential and a long-range attractive tail. Later contributions in the same area are those of Sadr-Lahijany *et al.* [64] and of Franzese *et al.* [65].

Lee and Swendsen [9] have presented a simple model of liquid–liquid phase transitions based on a Lennard–Jones interaction. However, this is modified to reflect the possibility of different types of short range orientational order in materials in which such a LLPT may occur. Their model then indeed leads to a transition between high- and low-density liquids (HDL and LDL).

To model (of course, very schematically) effects of local ordering, Lee and Swendsen [9] represent the different relative local orientations with a spin-one-half variable. Then interactions between particles with the same spin are taken to be given by the original Lennard–Jones 6–12 form

$$\phi_{\uparrow\uparrow}(r) = \phi_{\downarrow\downarrow}(r) = 4\epsilon\left(\frac{\sigma_\ell^{12}}{r^{12}} - \frac{\sigma_\ell^6}{r^6}\right), \tag{A3}$$

while interactions between particles having opposite spins are taken to be purely repulsive, namely

$$\phi_{\downarrow\uparrow}(r) = \phi_{\uparrow\downarrow}(r) = 4\epsilon\left(\frac{\sigma_u^{12}}{r^{12}}\right). \tag{A4}$$

It turns out that some properties are sensitive to the relative values of the 'diameters' σ_ℓ and σ_u appearing in the forms (A3) and (A4). In particular, a LLPT occurs when $\sigma_u < \sigma_\ell$, so that by spin re-orientation the particles may acquire different coordination numbers and local structures, as for example in liquid C discussed in some detail in Section 3 above.

The above model can be modified, as stressed by Lee and Swendsen [9], to couple to a (fictitious) external magnetic field. If one defines the magnetic moment as the sum of all spins, then the Hamiltonian may be written as

$$H = \frac{1}{2}\sum_{i\neq j}\phi_{ij}(r_{ij}) - h\sum_i \sigma_i \tag{A5}$$

h representing the magnetic field, and $\sigma_i = \pm 1$ is the direction of the spins of the particles. In the simulations reported by Lee and Swendsen [9], h is taken to be zero. Also units $T^* = k_B T/\epsilon$, $p^* = \sigma_\ell^2 k_B p/\epsilon$ were employed, while these authors set the cut-offs of the potential at $3\sigma_\ell$.

Monte Carlo simulations, reported in [9], were then carried out on the two-dimensional version of the above model, though the model itself is not limited to two dimensions. Various ensembles were employed in their simulations. Though simulations proved difficult, necessitating an extension of the customary techniques, clear evidence

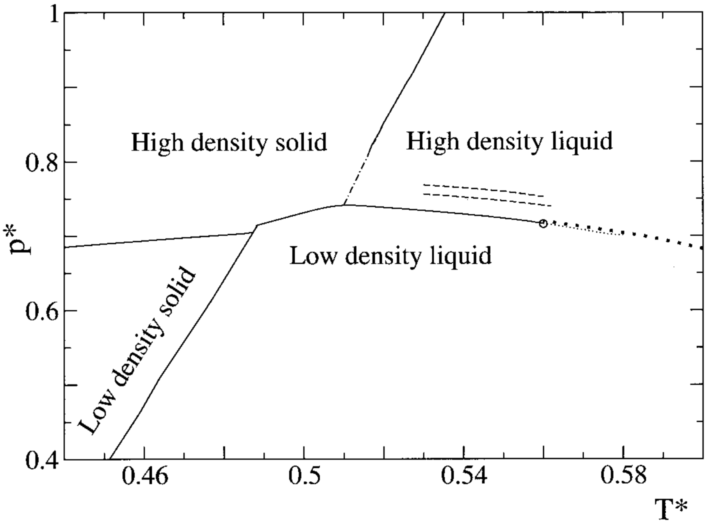

FIGURE 10 *p–T* diagram in Lee–Swendsen model of LLPT [9]. Solid lines show coexistence curves obtained from simulations with 160 particles. The circle marks shows the tricritical point. Redrawn from Lee and Swendsen [9].

was presented in [9] of a LLPT at high pressures. It proved feasible to map out both *p–T* and *p–ρ* phase diagrams.

The *p–T* diagram thus obtained by Lee and Swendsen is presented in Fig. 10, redrawn from their work. The solid lines show the coexistence curves they obtained from simulations with 160 particles. The boundary separating a HDL from a LDL is quite evident. One point emphasized by Lee and Swendsen is the negative slope of the liquid–liquid coexistence line in their model, which reflects the high entropy in the HDL phase. They point out that such a feature is found in most, but not all, materials exhibiting a LLPT. One exception is found in the phase diagram of C as determined by Glosli and Ree [4], and reported in Section 3.